

# Temperature-Induced Momentum-Dependent Spectral Weight Transfer in $\text{Bi}_2\text{Sr}_2\text{CaCu}_2\text{O}_{8+\delta}$

Z.-X. Shen, P. J. White, D. L. Feng, C. Kim, G. D. Gu, H. Ikeda, R. Yoshizaki, N. Koshizuka

Angle-resolved photoemission data from the cuprate superconductor  $\text{Bi}_2\text{Sr}_2\text{CaCu}_2\text{O}_{8+\delta}$  above and below the superconducting transition temperature  $T_c$  reveal momentum-dependent changes that extend up to an energy of about 0.3 electron volt, or  $40kT_c$  (where  $k$  is the Boltzmann constant). The data suggest an anomalous transfer of spectral weight from one momentum to another, involving a sizable momentum transfer  $\mathbf{Q} \sim (0.45\pi, 0)$ . The observed  $\mathbf{Q}$  is intriguingly near the charge-order periodicity required if fluctuating charge stripes are present.

In a conventional superconductor,  $T_c$  is regulated by the superconducting energy gap  $\Delta$ , which is related to the characteristic phonon energy (1). The central physics can be described with a mean-field approach, as in the theory of Bardeen, Cooper, and Schrieffer (BCS) (2). In this paradigm, only excitations near  $\Delta$  out from the available Fermi energy  $E_F$  are modified by superconductivity. The phase-space constraint imposed by these two drastically different energy scales, a few thousandths of an electron volt for  $\Delta$  and a few electron volts for  $E_F$ , limits an electron with momentum  $\mathbf{k}$  to mix only with electrons with momenta near  $\mathbf{k}$  and  $-\mathbf{k}$  through the coherence factors (1).

We report angle-resolved photoemission spectroscopy (ARPES) data from optimally doped  $\text{Bi}_2\text{Sr}_2\text{CaCu}_2\text{O}_{8+\delta}$  single crystals that suggest a different paradigm in high- $T_c$  superconductors. As the temperature is lowered from above to well below  $T_c$ , the single-particle excitation spectra show changes that strongly depend on  $\mathbf{k}$ . At certain momenta, the change extends up to an energy close to 300 meV, or  $40kT_c$ , much larger than the BCS value near  $2kT_c$ . Furthermore, spectral weight is transferred from very high energy at a momentum  $\mathbf{k}$  to a much lower energy at another momentum  $\mathbf{k}'$  that is far from either  $\mathbf{k}$  or  $-\mathbf{k}$ . Along the  $(1, 0)$  direction, the momentum-dependent spectral weight transfer seems to broadly peak near  $|\mathbf{Q}| \sim 0.45\pi$ . This  $\mathbf{Q}$ , and the previously found collective excitations of similar energy scale but with a different

momentum transfer  $\mathbf{Q}'$  broadly peaked near  $(\pi, \pi)$  (3), are intriguingly close to the charge- and spin-order periodicities that are required if the fluctuating charge stripes are present.

In an ARPES experiment, a monochromatic photon beam ejects photoelectrons whose energy and momentum are analyzed by an electron spectrometer (4). Special attention is paid during the experiment to ensure the proper normalization of the data. The spectra above and below  $T_c$  were first normalized to the integrated signal intensi-

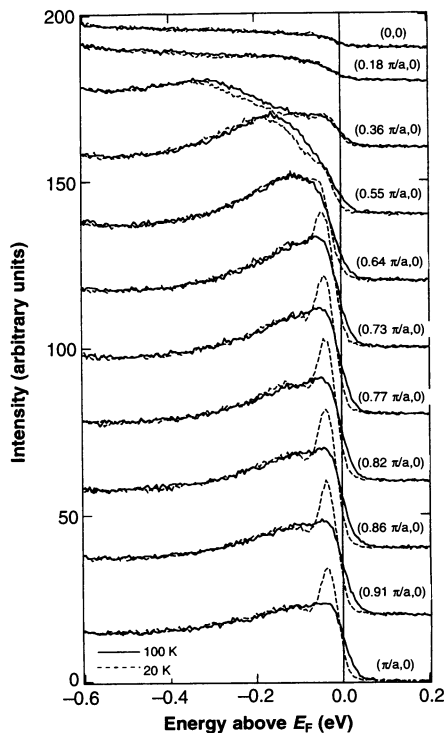


**Fig. 1.** Angle-resolved photoemission data along  $(0, 0)$  to  $(\pi, 0)$  from a  $\text{Bi}_2\text{Sr}_2\text{CaCu}_2\text{O}_{8+\delta}$  single crystal with  $T_c = 88$  K. The solid line gives data at 100 K, and the dashed line gives data at 20 K. The momenta are expressed in units of  $1/a$ , with  $a$  being the lattice constant.

ty above  $E_F$  that came from scattered electrons excited by higher order light and was roughly proportional to the angle-integrated spectral weight. For a given pair at each momentum, the spectra were further rescaled so that the high-binding-energy tails were also matched, consistent with the general expectation that the data above and below  $T_c$  should be the same at these energies. The latter procedure, which is needed probably because of subtle effects such as changes in sample position as a result of thermal expansion of the cryostat, involves only minor rescaling. The physics discussed here remains the same with or without the application of the second procedure.

In the normal state, a broad feature in the ARPES data along  $(0, 0)$  to  $(\pi, 0)$  (Fig. 1) was observed to disperse from  $-300$  meV near  $(0.36\pi, 0)$  to almost the Fermi level near  $(\pi, 0)$ . The dispersion is rapid from  $(0.36\pi, 0)$  to  $(0.64\pi, 0)$  but slow from  $(0.64\pi, 0)$  to  $(\pi, 0)$  (5). In the superconducting state (Fig. 1), a sharp peak emerges from the broad normal-state feature with a dip at higher energy, although the dip is weaker than typically seen (6). The most important observation emphasized here is the strong temperature-induced  $\mathbf{k}$ - and  $E$ -dependent spectral weight transfer. Although the overall spectral weight appears to gain slightly near  $(\pi, 0)$ , spectral weight is lost upon the superconducting transition at momenta  $(0.36\pi, 0)$  and  $(0.55\pi, 0)$ . Furthermore, the spectral weight loss extends up to a remarkably high energy of 300 meV at  $(0.36\pi, 0)$ . However, the slight gain of spectral weight from  $(0.73\pi, 0)$  to  $(\pi, 0)$  remains concentrated at the low-binding-energy portion.

Figure 2 plots the frequency-integrated spectral weight difference above and below  $T_c$  as a function of  $\mathbf{k}$ . The quantity  $A_{sc} -$

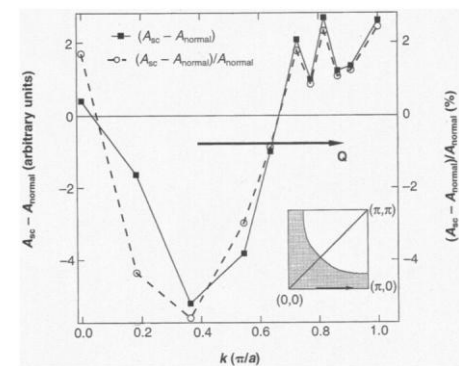


**Fig. 2.** Momentum-dependent spectral weight change along  $(0, 0)$  to  $(\pi, 0)$ . The data show that the spectral intensity is transferred from one momentum to another, with a transferring vector  $\mathbf{Q}$  broadly peaking between  $0.4\pi$  and  $0.5\pi$ . (Inset) The expected Fermi surface. The shaded area depicts the occupied states.

Z.-X. Shen, P. J. White, D. L. Feng, C. Kim, Department of Applied Physics, Department of Physics, and Stanford Synchrotron Radiation Laboratory, Stanford University, Stanford, CA 94305, USA.

G. D. Gu, School of Physics, The University of New South Wales, Post Office Box 1, Kensington, New South Wales 2033, Australia.

H. Ikeda and R. Yoshizaki, Institute of Applied Physics and Cryogenics Center, University of Tsukuba, Tsukuba, Ibaraki 305, Japan.

N. Koshizuka, Superconductivity Research Laboratory, ISTEC, 10-13 Shinonome, 1-chome, Koto-ku, Tokyo 135, Japan.

$A_{\text{normal}}$ , where  $A$  is the  $\mathbf{k}$ -resolved single-particle spectral weight, when normalized to the normal-state value  $A_{\text{normal}}$ , gives the difference of the occupation probabilities in the two states,  $[n_{\mathbf{k}}(s) - n_{\mathbf{k}}]/n_{\mathbf{k}}$  [here  $n_{\mathbf{k}}$  and  $n_{\mathbf{k}}(s)$  represent the occupation probabilities of the normal and superconducting states, respectively]. The data make clear that spectral weight is transferred from one  $\mathbf{k}$  to another  $\mathbf{k}'$ . The gain in spectral weight for one  $\mathbf{k}$  and loss at another  $\mathbf{k}'$  is consistent with the sum rule requiring that the  $\mathbf{k}$ -integrated spectral weight, which is proportional to the particle number, be conserved (7). The detailed balance of  $\mathbf{k}$ -integrated spectral weight requires considerations of other factors, such as photoionization cross section and the phase-space volume. It appears that the spectral weight is transferred by a  $\mathbf{Q} \sim (0.45\pi, 0)$  for the following reasons. Among the high-symmetry directions we have investigated— $(0, 0)$  to  $(\pi, 0)$ ,  $(\pi, 0)$  to  $(\pi, \pi)$ , and  $(0, 0)$  to  $(\pi, \pi)$  (Fig. 2, inset)—the  $\mathbf{k}$ -dependent spectral weight transfer is strongest along the  $(0, 0)$  to  $(\pi, 0)$  direction. Along  $(0, 0)$  to  $(\pi, 0)$ ,  $(A_{\text{sc}} - A_{\text{normal}})/A_{\text{normal}}$  gives a negative minimum near  $0.4\pi$  and smaller positive values from  $0.7\pi$  to  $\pi$ . Considering that the spectral weight should be conserved within the first Brillouin zone, the most reasonable  $|\mathbf{Q}|$  should connect the minimum at  $0.4\pi$  to the middle of  $0.7\pi$  and  $\pi$ , yielding a value of  $(0.7\pi + \pi)/2 - 0.4\pi = 0.45\pi$ . Within this scheme, the uncertainty in  $|\mathbf{Q}|$  stems more from the maximum of  $(A_{\text{sc}} -$

$A_{\text{normal}})/A_{\text{normal}}$ , as it is very broad. Indeed, the small amount of the spectral weight gain is close to the experimental uncertainty. Despite these uncertainties of finer details, the general feature of the  $\mathbf{k}$ -dependent spectral weight transfer as a function of temperature is apparent in the raw data (Fig. 1). This finding deviates strongly from the BCS paradigm.

According to the BCS theory for phonon-mediated superconductors (1, 8) (Fig. 3), for electrons in the Fermi sea, only a small shell of excitations up to the characteristic phonon energy  $\hbar\nu_{\text{phonon}}$  away from the Fermi energy is possible ( $\hbar$  is the Planck constant,  $\nu$  is the phonon frequency). For two electrons with momenta  $\mathbf{k}_1$  and  $\mathbf{k}_2$ , an exchange of a virtual phonon will yield electrons with momenta  $\mathbf{k}_1'$  and  $\mathbf{k}_2'$ . The total momentum  $\mathbf{k}_1 + \mathbf{k}_2 = \mathbf{k}_1' + \mathbf{k}_2' = \mathbf{K}$  is conserved, requiring that only the shaded phase-space region in Fig. 3B is available for this interaction. Because the typical value of  $\hbar\nu_{\text{phonon}}/E_F$  is about  $10^{-2}$  to  $10^{-3}$ , the phase space spanned by  $\Delta\mathbf{k}$  is small, except when  $\mathbf{K} = 0$ . Thus, the pairing interaction in a superconducting condensate is dominated by electrons with opposite momentum,  $\mathbf{k}_1 = -\mathbf{k}_2$ . In a similar fashion, only the electron excitations within a shell of  $\Delta$  will be modified. Depending on the electron-phonon coupling constant,  $\Delta$  can be even smaller than  $\hbar\nu_{\text{phonon}}$ . In a single-particle spectral function measured by ARPES, one should only see an upward shift of the electron energy from its normal-

state value  $\epsilon_{\mathbf{k}}$  to  $(\epsilon_{\mathbf{k}}^2 + \Delta^2)^{1/2}$ . This energy renormalization is significant only when  $\epsilon_{\mathbf{k}}$  is smaller and comparable to  $\Delta \sim 2kT_c$  (Fig. 3A). The shaded area in Fig. 3C depicts the change in occupation probability from that in the normal state ( $n_{\mathbf{k}}$ ) to that in the superconducting state [ $n_{\mathbf{k}}(s)$ ]. In the superconducting state, the occupation probability is modified according to the superconducting coherence factor

$$v_{\mathbf{k}} = \frac{1}{2} \left[ 1 - \frac{\epsilon_{\mathbf{k}}}{(\epsilon_{\mathbf{k}}^2 + \Delta^2)^{1/2}} \right]^{1/2} \quad (1)$$

which stems from the quasiparticle in the superconducting state being a mixture of an electron and a hole. This factor should always be smaller than 1 for occupied states along  $(0, 0)$  to  $(\pi, 0)$ .

The energy scale of 300 meV, or  $40kT_c$ , is much higher than the expected BCS value of about  $2kT_c$  (1). In the strong-coupling BCS-Eliashberg theory (1), one may see very weak temperature-dependent changes due to phonons whose energies are higher than  $\Delta$ . Although changes up to very high energies have been observed in cuprates by other techniques, they are evidently related to the dispersion (Fig. 1), ruling out the phonons as a possible explanation. Because the change extends up the entire dispersion of the band or the "bandwidth  $\sim E_F$ ," which is regulated by the exchange coupling constant  $J$  (9, 10), there is no hierarchy of energy scales in the system. Instead of having only a small energy window  $\Delta$  out of  $E_F$  being available for pairing interactions, the whole bandwidth of scale  $E_F$  is available (Fig. 3, D and E). This expanded window would probably mean that, instead of only the small fraction of electrons near  $E_F$ , all electrons are involved in the pairing interaction (11). A corollary of the above observation would be that  $T_c$  may be limited by factors other than the strength of the pairing interaction. This idea is consistent with a growing indication that the superconducting transition may not be described by a mean-field theory like BCS (12), especially for the underdoped cuprate superconductors. Within the context of ARPES data, the lack of scaling of  $\Delta$  with  $T_c$  (13) and the existence of the pseudogap in the normal state (14) are consistent with this view.

In addition to the high energy scale involved, perhaps more striking is the anomalous  $\mathbf{k}$ -dependent spectral weight transfer above and below  $T_c$ . The occupation probability below  $T_c$  goes above the normal-state value from  $(0.7\pi, 0)$  to  $(\pi, 0)$  (Fig. 3F), violating the BCS picture (Fig. 3C), requiring it to be smaller than the normal-state value. This probability appears to come from the  $\mathbf{k}$ -space region that is  $\mathbf{Q}$

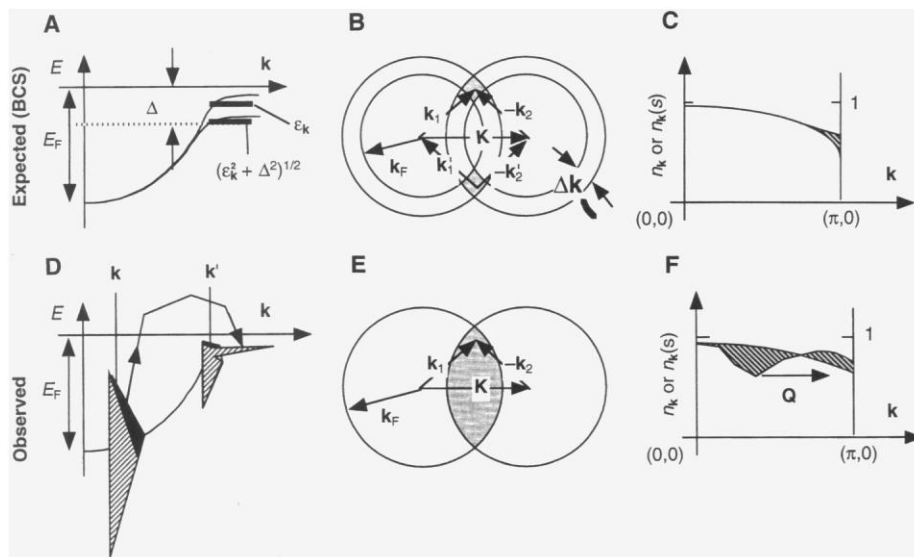


**Fig. 3.** Schematic comparison between (A through C) BCS theory and (D through F) the observed result. (A) Quasiparticle band diagram and expected energy position at  $\epsilon_{\mathbf{k}}$  and  $(\epsilon_{\mathbf{k}}^2 + \Delta^2)^{1/2}$  above and below  $T_c$ , respectively. (B) Allowed phase space (shaded area) for pairing interaction of electrons  $\mathbf{k}_1$  and  $\mathbf{k}_2$ . (C) Occupation probability. The shaded area is the reduction below  $T_c$ . (D) Spectral weight transfer from  $\mathbf{k}$  at higher energy to various  $\mathbf{k}'$  at lower energy, in contrast to (A). (E) The relaxed phase-space constraint (shaded area). (F) Measured occupation probabilities, which is the frequency-integrated spectral weight. The shaded area is the difference above and below  $T_c$ .

away. Furthermore, the result depicted in Fig. 3D implies that the anomalous excess spectral weight at  $\mathbf{k}'$  actually comes from much higher energy at another  $\mathbf{k}$ , although the spectral weight at each  $\mathbf{k}$  shifts toward higher energy as the sample is cooled below  $T_c$ . Given such a large value of  $|\mathbf{Q}|$ , the  $\mathbf{k}$ -dependent spectral weight transfer is not caused by the mixing of states with momenta close to  $\mathbf{k}$  and  $-\mathbf{k}$ .

There are several possible non-BCS interpretations of the data. The observed  $\mathbf{q}$  structure can be readily explained if the system has collective excitations, which have real-space periodicities corresponding to  $\mathbf{Q}$ , that are enhanced or developed at lower temperature. The question is the origin of these excitations, which is obviously not the Bi-O superstructure, which has a very different  $\mathbf{q}$  value. An earlier observation indicated that the system has other collective excitations with  $\mathbf{Q}' \sim (\pi, \pi)$  (3). It is intriguing that  $\mathbf{Q}$  and  $\mathbf{Q}'$  are close to the expected momenta of charge and spin ordering in the charge stripes that were first observed in neutron scattering from  $\text{La}_{1.48}\text{Nd}_{0.4}\text{Sr}_{0.12}\text{CuO}_4$  (15). The stripe model envisages the doped holes segregating into domain walls (stripes) that separate antiferromagnetic regions with a phase slip of  $\pi$  across a domain wall (antiphase domains). The model requires the existence of a charge-order peak at  $\mathbf{q} = (\pm 2x, 0)2\pi$  or  $(0, \pm 2x)2\pi$  and a spin-order peak at  $\mathbf{q}' = (\pi, \pi \pm x\pi)$  or  $(\pi \pm x\pi, \pi)$ , with  $x$  being the doping level. The neutron peak at  $\mathbf{q}'$  seen in  $\text{La}_{1.48}\text{Nd}_{0.4}\text{Sr}_{0.12}\text{CuO}_4$  is of elastic nature, making the identification of the stripe correlation unambiguous. However, earlier neutron experiments from  $\text{La}_{2-x}\text{Sr}_x\text{CuO}_4$  samples of lower doping have also identified inelastic peaks near the same  $\mathbf{q}'$  (16). It has been argued that the inelastic peaks are caused by dynamic stripe correlations (15). A recent doping-dependent study of  $\text{La}_{2-x}\text{Sr}_x\text{CuO}_4$  found that  $\mathbf{q}'$  stops deviating further from  $(\pi, \pi)$  when  $x$  is increased to near  $1/8$  (17). The presence of the stripe correlation has also been predicted theoretically (18, 19). Recently, it was found that the spacing between the  $(1, 0)$  domain walls, which decreases with doping for  $x < 1/8$ , saturates with  $x$  near  $1/8$ , and the situation becomes more complicated for  $x > 1/8$  (20). Taking the nominal number of  $\delta \sim 0.18$  near optimal doping (21), we use the saturated value of  $x = 1/8$  and  $\mathbf{q} = (\pm 0.5\pi, 0)$  or  $(0, \pm 0.5\pi)$  and  $\mathbf{q}' = (\pi, \pi \pm 0.12\pi)$  or  $(\pi \pm 0.12\pi, \pi)$ . These momenta are intriguingly close to the observed  $\mathbf{Q} \sim (0.45\pi, 0)$  and  $\mathbf{Q}' \sim (\pi, \pi)$  if one recognizes the broadness of the  $\mathbf{q}$  structures.

Within the context of the above stripe interpretation, our data have important implications. First, the effect is observed in a

sample with a very high  $T_c$ , unlike the  $\text{La}_{1.48}\text{Nd}_{0.4}\text{Sr}_{0.12}\text{CuO}_4$  case, where  $T_c$  is strongly suppressed (15). Therefore, the stripe correlations coexist with high- $T_c$  superconductivity. The stripe correlations are short ranged, as reflected in the broadness of the  $\mathbf{q}$  structure. Further, because the spectral weight transferred by  $\mathbf{Q}$  comes from high to low energies (Fig. 1), the scattering process is energy-dependent, again suggesting the dynamic nature of the stripes. This picture is consistent with a theoretical model proposed by Emery, Kivelson, and Zachar connecting the presence of fluctuating stripes and high- $T_c$  superconductivity (11). Second, the data provide complementary information about the stripe correlation. To date, the most important experimental evidence for stripe correlation stems from neutron scattering experiments, which are most sensitive to the spin order. The information about charge order stems indirectly from the nuclear superlattice peaks seen in neutron scattering (15), x-ray scattering (22), and extended x-ray absorption fine structure experiments (23). The photoemission data provide more direct information for the valence-charge distribution. Further, the observed change up to 300 meV, which is an energy scale controlled by  $J$  (9, 10), suggests that the stripe phenomenon is related to the strong antiferromagnetic interactions. This result is consistent with several theoretical studies using many-body models (11, 18–20). Third, the stripe interpretation implies that the spectral weight transfer between data recorded at 20 K and those at 100 K may not be a direct product of superconductivity. The spectral change above and below  $T_c$  may merely facilitate the identification of the stripe correlations that are gradually enhanced at lower temperatures. Having identified the stripes, ARPES may be used to study the issue of whether the stripes facilitate or compete with superconductivity.

The above interpretation is the most plausible explanation of our data, but more experiments are needed to further check this interpretation. The most obvious check will be the results from underdoped samples, but this will be a challenging experiment because the surfaces of underdoped samples are very reactive, making it hard to get reliable temperature-dependent data with sufficient statistics to see the subtle effects in Fig. 1, even in an extremely good vacuum. Finally, we need to test our data against other theoretical models. For example, the change at  $(0.36\pi, 0)$  and  $(0.55\pi, 0)$  may alternatively be interpreted as a shift of the broad feature, as discussed for boson pairs (24).

The possible presence of the stripes may shed light on the long-standing problem regarding the photoemission line shape

(25). Given the stunningly sharp peak seen below  $T_c$ , the extremely broad feature in the normal state reflects a completely incoherent motion. The anomalously strong scattering may be directly related to the material's propensity to have a microscopically inhomogeneous charge distribution because they are manifestations of the same underlying interactions. This propensity of inhomogeneity is also in concert with the spectral line shape in the superconducting state. Below  $T_c$ , the spectra may be broken into two parts, representing the two corresponding electronic components. The first is the sharp peak that represents the superfluid density (26); the second is a higher energy portion of the spectra that is as broad as those of the normal state. Both components appear to be important for superconductivity because  $T_c$  scales with the first in the underdoped regime (13) and the pairing strength correlates with the second in the overdoped regime (3, 27). Within the context of a recent theory (11), the first component arises from the carriers of the hole-rich region, and the second arises from those in the hole-poor region. This assignment is consistent with the first component scaling with doping and with the second component being similar to spectra from an antiferromagnetic insulator (28) and providing pairing interactions that peak near  $(\pi, \pi)$  (3). The growth of the first component at the expense of the low-energy portion of the second component (Fig. 1) suggests that electrons change their allegiance to the two components dynamically. The coexistence of stripes and superconductivity helps to visualize the two-component picture. However, the phenomenology itself does not require the electronic components to form regular arrays. Thus, the next experimental challenge will be to investigate whether the stripes are merely windows that reveal the secret of the underlying interactions or are the intermediate steps leading to the high  $T_c$ . Independent of its outcome, the physical picture that has emerged here calls for a far-reaching revision of our ideas of metals and superconductors.

## REFERENCES AND NOTES

1. J. R. Schrieffer, *Theory of Superconductivity* (Addison-Wesley, New York, 1988).
2. J. Bardeen, L. N. Cooper, J. R. Schrieffer, *Phys. Rev.* **106**, 162 (1957); *ibid.* **108**, 1175 (1957).
3. Z.-X. Shen and J. R. Schrieffer, *Phys. Rev. Lett.* **78**, 1771 (1997).
4. Spectra were recorded with a chamber attached to beamline 5-3 of the Stanford Synchrotron Radiation Laboratory. The total energy resolution was typically 35 meV, and the angular resolution was  $\pm 1^\circ$ . The nominal chamber pressure during the measurement was  $3 \times 10^{-11}$  to  $5 \times 10^{-11}$  torr, and the photon energy used was 22.4 eV. At this photon energy, the data approximate the momentum-resolved single-particle spectral weight function  $A(\mathbf{k}, \omega)$ . Our high-quality single crystals were grown by the traveling-

- floating-zone method. Some of these crystals were used as reference samples for systematic doping studies using Fe, Zn, and Ni [G. D. Gu *et al.*, *J. Cryst. Growth* **130**, 325 (1993); *ibid.* **137**, 472 (1994); D.-S. Jeon *et al.*, *Physica C* **253**, 102 (1995)]. The data presented here were obtained from a sample with  $T_c = 88$  K, near optimal in the  $\text{Bi}_2\text{Sr}_2\text{CaCu}_2\text{O}_{8+x}$  system. The results were reproduced in three samples from the same growth batch by Gu and colleagues. The spectra from these samples show a systematic set of subtle but important differences from other samples that we have used before [D. B. Mitzi *et al.*, *Phys. Rev. B* **41**, 6564 (1990)]. The details of these differences, their relation to the effects reported here, and the implications will be published elsewhere.
5. D. S. Dessau *et al.*, *Phys. Rev. Lett.* **71**, 2781 (1993).
  6. D. S. Dessau *et al.*, *ibid.* **66**, 2160 (1991); Y. Hwu *et al.*, *ibid.* **67**, 2573 (1991); M. Norman *et al.*, *ibid.* **79**, 3506 (1997).
  7. M. Randeria *et al.*, *ibid.* **74**, 4951 (1995).
  8. H. Ibach and H. Luth, *Solid-State Physics* (Springer, New York, 1995).
  9. For an overview, see R. B. Laughlin, *J. Phys. Chem. Solids* **56**, 1627 (1995); A. Moreo *et al.*, *ibid.*, p. 1645; R. Preuss *et al.*, *ibid.*, p. 1659; Y. Ota *et al.*, *ibid.*, p. 1741.
  10. R. B. Laughlin, *Phys. Rev. Lett.* **79**, 1726 (1997).
  11. V. J. Emery, S. A. Kivelson, O. Zachar, *Phys. Rev. B* **56**, 6120 (1997); *Physica C* **282-287**, 174 (1997).
  12. B. G. Levi, *Phys. Today* **49** (no. 6), 17 (1996).
  13. J. M. Harris *et al.*, *Phys. Rev. B* **54**, R15665 (1996).
  14. D. S. Marshall *et al.*, *Phys. Rev. Lett.* **76**, 4841 (1996); A. G. Loeser *et al.*, *Science* **273**, 325 (1996); H. Ding *et al.*, *Nature* **382**, 51 (1996).
  15. J. M. Tranquada *et al.*, *Nature* **375**, 561 (1995).
  16. S. W. Cheong *et al.*, *Phys. Rev. Lett.* **67**, 1791 (1991); T. E. Mason *et al.*, *ibid.* **68**, 1414 (1992); T. R. Thurston *et al.*, *Phys. Rev. B* **46**, 9128 (1992).
  17. K. Yamada *et al.*, in preparation.
  18. H. J. Schultz, *J. Phys. (Paris)* **50**, 2833 (1989).
  19. D. Poilblanc and T. M. Rice, *Phys. Rev. B* **39**, 9749 (1989); J. Zaanen and O. Gunnarson, *ibid.* **40**, 7391 (1989); S. A. Kivelson and V. J. Emery, *Physica C* **235-240**, 189 (1994).
  20. S. R. White and D. J. Scalapino, cond-mat/9801274, Los Alamos e-Print Archive at xxx.lanl.gov (1998).
  21. W. A. Groen, D. M. de Leeuw, L. F. Feiner, *Physica C* **165**, 55 (1990).
  22. M. V. Zimmermann *et al.*, *Europhys. Lett.*, in press.
  23. A. Bianconi *et al.*, *Phys. Rev. Lett.* **76**, 3412 (1996).
  24. X.-G. Wen and P. A. Lee, cond-mat/9709108, Los Alamos e-Print Archive at xxx.lanl.gov (1997).
  25. G. A. Sawatzky, *Nature* **342**, 480 (1989); P. W. Anderson, *Phys. Rev. Lett.* **67**, 2569 (1991).
  26. Although ARPES only measures the single-particle spectral function, this connection is empirically justified because its strength correlates with  $T_c$  (27) and  $T_c$  scales with superfluid density (29) in the underdoped regime.
  27. P. J. White *et al.*, *Phys. Rev. B* **54**, R15669 (1996).
  28. B. O. Wells *et al.*, *Phys. Rev. Lett.* **74**, 964 (1995).
  29. Y. J. Uemura, in *Proceedings of the CCAST Symposium on High- $T_c$  Superconductivity and C60 Family*, Beijing, 1994, S. Feng and H. C. Ren, Eds. (Gordon & Breach, New York, 1995), pp. 113-142.
  30. We acknowledge S. A. Kivelson, S.-C. Zhang, R. B. Laughlin, A. Puchkov, Z. Hasan, P. A. Lee, A. J. Millis, P. Coleman, and G. A. Sawatzky for helpful discussions. Photoemission experiments were performed at the Stanford Synchrotron Radiation Laboratory, which is operated by the U.S. Department of Energy's Office of Basic Energy Science, Division of Chemical Sciences. The Office's Division of Material Science provided support for this research.

18 December 1997; accepted 20 February 1998

## Optical Studies of Individual InAs Quantum Dots in GaAs: Few-Particle Effects

L. Landin, M. S. Miller,\* M.-E. Pistol,†  
C. E. Pryor, L. Samuelson

Optical emission from individual strained indium arsenide (InAs) islands buried in gallium arsenide (GaAs) was studied. At low excitation power density, the spectra from these quantum dots consist of a single line. At higher excitation power density, additional emission lines appeared at both higher and lower energies, separated from the main line by about 1 millielectron volt. At even higher excitation power density, this set of lines was replaced by a broad emission peaking below the original line. The splittings were an order of magnitude smaller than the lowest single-electron or single-hole excited state energies, indicating that the fine structure results from few-particle interactions in the dot. Calculations of few-particle effects give splittings of the observed magnitude.

Semiconductor quantum dots have been the subject of intense research in recent years. These heterostructures consist of nanometer-scale islands of one type of semiconductor either embedded in a different semiconductor or free-standing on a suitable substrate. The materials are chosen such that electrons and holes are confined to the island, resulting in a discrete spectrum for the confined charges. The spectrum of a quantum dot provides information about its internal structure, similar to the spectrum of an atom or a molecule. Unlike atoms and molecules, however, quantum dots suffer from unavoidable variation in their size, and hence, their energy levels. Previous measurements most often averaged

over many dots, making it difficult to disentangle the features related to single-dot physics from those arising from dot-to-dot variation.

Recent studies of individual semiconductor quantum dots showed departures from a single-particle description of quantum dots, using magnetoconductance measurements (1) and differential conductance measurements (2). In these studies, the quantum dots were filled with only one type of charge carrier (electrons), leading to strong Coulomb effects. Studies of photon emission from localized sites arising from interface fluctuations in quantum wells showed the existence of excitons (3, 4) and bi-excitons (4), which consist of two different types of charge carriers, electrons and holes. Tri-excitons have been observed in the CuCl system (5). Even studies of individual pairs of quantum dots have been performed, showing clear effects of coupling between the quantum dots (6). We expect that studies of individual quantum dots will

become increasingly important in the near future, similar to the situation with single-molecule studies (7). The relative ease of positioning of quantum dots, in comparison with single atoms (for which atomic traps are needed), will facilitate experiments in quantum computing (8), to use one example. In such experiments, it will be necessary to control the electronic states of the quantum dots using, for example, fast pulsed lasers.

One extensively studied quantum dot system is InAs islands embedded in GaAs. Indium arsenide has a 7.2% larger lattice constant than GaAs, and only a thin layer of InAs can be grown on a GaAs surface before the film breaks up into small islands on a thin InAs wetting layer (9). When embedded in GaAs, the InAs islands are small enough to confine the electronic states strongly in all three dimensions, making good quantum dots with low-temperature luminescence energies between 1.0 and 1.4 eV. The wetting layer behaves as a thin quantum well. Several groups have formed such islands on flat substrates, using molecular beam epitaxy (10-12), metal-organic chemical vapor deposition (13, 14), and chemical beam epitaxy (15). The optical emission spectra of individual dots are of great interest, because the spectra characterize the electronic structure and thus determine the properties available for optical or electrical device applications. Recently, optical emission spectra for individual InP quantum dots in barriers of GaInP were reported to have multiple emission lines for each InP dot even at low excitation power density (16). The InP dot spectral features were in good agreement with detailed electronic structure calculations (17). Spectra with narrow emission lines from small numbers of InAs dots in GaAs (12, 18, 19) have

Department of Solid State Physics, Lund University, Box 118, S-221 00 Lund, Sweden.

\*Present address: Department of Electrical Engineering, University of Virginia, Thornton Hall, Charlottesville, VA 22903-2442, USA.

†To whom correspondence should be addressed. E-mail: mats-erik.pistol@tf.fth.se